

## Functional MRI Measurements to Predict Early Adenoviral Gene Therapy Response in Ovarian Cancer Mouse Model

Tuppurainen L<sup>1</sup>, Sallinen H<sup>1,2,3</sup>, Hakkarainen H<sup>1,4</sup>, Liimatainen T<sup>1,4</sup>, Hassan M<sup>1</sup>, Ylä-Herttuala E<sup>1,4</sup>, Anttila M<sup>1,2,3</sup>, Hämäläinen K<sup>2,5</sup>, Veli-Matti Kosma<sup>2,5</sup>, Heinonen S<sup>2,3</sup>, Alitalo K<sup>6</sup> and Ylä-Herttuala S<sup>1,7,8\*</sup>

<sup>1</sup>Department of Biotechnology and Molecular Medicine, A.I. Virtanen Institute for Molecular Sciences, University of Eastern Finland, Kuopio, Finland

<sup>2</sup>Institute of Clinical Medicine, Gynecology, and Pathology and Forensic Medicine, University of Eastern Finland, Kuopio, Finland

<sup>3</sup>Department of Gynecology, Kuopio University Hospital, Kuopio, Finland

<sup>4</sup>Cardiovascular Imaging Group, A. I. Virtanen Institute for Molecular Sciences, University of Eastern Finland, Kuopio, Finland

<sup>5</sup>Department of Pathology, Kuopio University Hospital, Kuopio, Finland

<sup>6</sup>Molecular/Cancer Biology Laboratory Biomedicum Helsinki and Haartman Institute, University of Helsinki, Helsinki, Finland

<sup>7</sup>Gene Therapy Unit, Kuopio University Hospital, Kuopio, Finland

<sup>8</sup>Research Unit, Kuopio University Hospital, Kuopio, Finland

### Abstract

Anti-angiogenic and anti-lymphangiogenic gene therapy is a new potential method for the treatment of epithelial ovarian carcinoma. We studied the usefulness and feasibility of diffusion-weighted magnetic resonance imaging (DW-MRI) and relaxation measurements as surrogate markers of AdsVEGFR-2, AdsVEGFR-3, AdsNRP-1 and AdsNRP-2 gene therapy treatment responses in an intraperitoneal ovarian cancer mouse model (n= 40). Gene therapy was also combined with paclitaxel and carboplatin chemotherapy. Gene therapy was performed when visible tumors were noticed in MRI. Adenoviral gene transfer was dosed intravenously ( $2 \times 10^9$  pfu), while chemotherapy was dosed intraperitoneally. The study groups were: AdLacZ as controls (group I); AdsVEGFR-2 and AdsVEGFR-3 (group II); combination of AdsVEGFR-2, AdsVEGFR-3 and chemotherapy (group III) and AdsNRP-1 and AdsNRP-2 (group IV). Antitumor effectiveness was assessed by sequential MRI, immunohistochemistry, microvessel density, overall tumor growth, formation of ascites and survival time. Early responses in tumor tissue were evaluated with MRI measurements using relaxation times  $T_2$ ,  $T_{1\rho}$ ,  $T_{RAFF2}$ ,  $T_{RAFF4}$  and water apparent diffusion coefficient (ADC). The mean survival of mice (30 days) was significantly prolonged in group II as compared to controls (24 days) or other treatment groups (p= 0.003). Microvessel density (MVD) and total vascular area (TVA) were significantly lower compared to controls in all groups: group II (p= 0.001), group III (p= 0.002), group IV (p= 0.026).  $T_2$  relaxation times were significantly increased at day 8 after the gene transfer in the combination gene therapy and chemotherapy group III compared to controls (p= 0.005). ADC values in the tumors were significantly increased in group IV at four days compared to controls (p= 0.044). Early changes in  $T_2$  relaxation times and ADC values after gene therapy suggest the potential of  $T_2$  relaxation time measurements and DW-MRI as early markers of treatment response after anti-angiogenic gene therapy and chemotherapy.

**Keywords:** Anti-angiogenesis; Chemotherapy; Diffusion-weighted MRI; Gene therapy; Ovarian cancer; Soluble VEGF-receptor; Soluble NRP-coreceptor

**Abbreviations:** Ad: Adenovirus; ADC: Apparent Diffusion Coefficient; DW-MRI: Diffusion-Weighted Magnetic Resonance Imaging; MVD: Microvessel Density; RAFF: Relaxation Along A Fictitious Field; sNRP: Soluble Neuropilin; sVEGFR: Soluble Vascular Endothelial Growth Factor Receptor; TVA: Total Vascular Area

### Introduction

Ovarian cancer is the most lethal gynecological cancer most often characterized by widely disseminated intraperitoneal carcinoma and ascitic fluid at the time of diagnosis. The mortality of ovarian cancer is highest in developed countries [1]. The 5-year survival rate of patients with disseminated cancer is only 19-47% despite cytoreductive surgery and chemotherapy [2]. New and more potent treatment methods are urgently required to improve the prognosis of patients with ovarian cancer [3].

In cancer the balance between pro- and anti-angiogenic growth factors has been disturbed in favor of angiogenesis [4]. Increased expression of proangiogenic vascular endothelial growth factors (VEGFs) is associated with poor prognosis and advanced stage of ovarian cancer [5,6]. VEGF family members (VEGF-A, -B, -C, -D and placental growth factors (PlGF)-1 and -2) are crucial in the

development of new capillaries, lymphatic vessels and metastasis of ovarian tumors [7]. VEGF- family members signal their angiogenic and lymphangiogenic effects in the cell through tyrosine kinase VEGF-receptors -1, -2 and -3, also known as Flt-1, KDR (or Flk-1) and Flt-4, respectively [8,9]. VEGFR-1 (binding VEGF-A, VEGF-B and PlGF) and VEGFR-2 (binding VEGF-A and processed forms of VEGF-C and VEGF-D) are considered as the major receptors of angiogenesis, vasculogenesis and vascular permeability [10,11]. VEGFR-3 binds VEGF-C and VEGF-D and is the most important receptor for lymphatic vessel formation thus contributing to tumor dissemination via the lymphatic system [12,13]. Neuropilin (NRP)-1

**\*Corresponding author:** Seppo Ylä-Herttuala, Professor of Molecular Medicine, A. I. Virtanen Institute, University of Eastern Finland, P.O.Box 1627, Kuopio, FIN-70211, Finland, Tel: +358 40 355 2075; E-mail: [Seppo.Ylaherttuala@uef.fi](mailto:Seppo.Ylaherttuala@uef.fi)

**Received** August 05, 2013; **Accepted** August 19, 2013; **Published** August 21, 2013

**Citation:** Tuppurainen L, Sallinen H, Hakkarainen H, Liimatainen T, Hassan M, et al. (2013) Functional MRI Measurements to Predict Early Adenoviral Gene Therapy Response in Ovarian Cancer Mouse Model. J Genet Syndr Gene Ther 4: 171. doi:[10.4172/2157-7412.1000171](https://doi.org/10.4172/2157-7412.1000171)

**Copyright:** © 2013 Tuppurainen L, et al. This is an open-access article distributed under the terms of the Creative Commons Attribution License, which permits unrestricted use, distribution, and reproduction in any medium, provided the original author and source are credited.

and NRP-2 are coreceptors for VEGFRs [14]. The mechanism of their signal transduction in angiogenesis is not completely understood [15]. Overexpression of NRP-1 and NRP-2 is indicated with many invasive cancers, including non-small cell lung carcinoma [16] and malignant glioma [17]. Since high expression of NRP-1 and NRP-2 correlate with cell proliferation, invasion and malignancy of ovarian cancer, they could provide additional therapeutic targets for ovarian cancer [18,19]. In this study, the combination of soluble VEGFR-2 and -3 alone or with chemotherapy and the combination of soluble NRP-1 and NRP-2 lacking their transmembrane and intracellular tyrosine kinase domains were used to inhibit the angiogenic and lymphangiogenic signaling in ovarian tumor tissue.

Due to necrosis and cavitation of tumor tissue, evaluation of treatment responses based on tumor size only as measured with traditional magnetic resonance imaging (MRI), is not an adequate method anymore. Thus, new molecular and functional imaging techniques have been developed to detect the treatment responses especially to targeted therapies [20]. In diffusion-weighted MRI (DW-MRI), water Brownian motion is in a key role to detect treatment responses, since necrosis and progression of tumor tissue will lead to alterations in water microscopic movement and consequently diffusion parameters [21]. Results from recent reports show that DW-MRI is a potential technique to assess the early treatment responses especially in cerebral applications [22-25]. In clinical ovarian cancer studies DW-MRI and calculation of apparent diffusion coefficient (ADC) values have been exploited to detect and characterize ovarian tumors and to measure treatment responses [23]. In our study, we have utilized a wide range of MRI parameters including relaxation times  $T_{1\rho}$ ,  $T_2$ ,  $T_{RAFF2}$  and  $T_{RAFF4}$  in addition to ADC values to monitor early gene therapy treatment responses in intraperitoneal ovarian carcinoma.

The aim of this study was to evaluate treatment responses of anti-angiogenic and anti-lymphangiogenic gene therapy with AdsVEGFR-2 and AdsVEGFR-3 alone and with chemotherapy (groups II and III) and AdsNRP-1 and AdsNRP-2 (group IV) in a human ovarian cancer xenograft model that closely mimics the complexity of tumor progression and shows a very aggressive behaviour [26]. As in our previous studies [27-29] morphologic MRI was used for the timing of gene therapy to treat sizeable tumors, not a micrometastatic disease. Furthermore, non-invasive DW-MRI and relaxation time measurements were used to monitor treatment responses at molecular level in several time points in solid ovarian cancer tumors. To our knowledge this is the first study to evaluate the use of DW-MRI and relaxation time measurements as early markers of anti-angiogenic gene therapy response in ovarian cancer. This study is also the first one to detect the efficacy of AdsVEGFR-2 and AdsVEGFR-3 gene therapy together with standard carboplatin and paclitaxel chemotherapy as well as AdsNRP-1 and AdsNRP-2 gene therapy in the ovarian cancer.

## Materials and Methods

### Cell line

Detailed characteristics of the used SKOV-3m ovarian cancer cell line have been described earlier [26]. Cells were cultured in McCoy's 5A medium (Sigma M8403, Steinheim, Germany). The cells were trypsinized and counted before in vivo inoculation. SKOV-3m cell line showed epithelial phenotype and resembled that of the original cell line.

### Viral vectors

Adenoviral serotype 5 vectors (replication-deficient E1-E3 deleted) were produced in 293 cells. Adenovirus encoding *LacZ* was used as a control vector [30]. Vectors for gene therapy were encoding human sVEGFR-2-IgG fusion protein [31], human sVEGFR-3-IgG [32], sNRP-1 and sNRP-2 [9,33]. Both sVEGFR constructs contain an immunoglobulin Fc domain to ensure efficient dimerization of the soluble decoy receptors. Adenoviruses were analyzed to be free of lipopolysaccharides, replication-competent viruses, and bacteriological contaminants [30,34].

### Animal model

In this study, seven to 12-weeks-old (n=40) Balb/cA-nu female nude mice were used. The mice were kept in a pathogen-free isolated unit at the National Experimental Animal Center of the University of Eastern Finland, Kuopio. The mice received chow and water *ad libitum*. Water, food and sawdust bedding were autoclaved. For the operations, animals were anesthetized with isoflurane (Isoflurane, Baxter Medical AB) (sleep; 4.5 % isoflurane and 450 ml air, upkeep; 1.7 % isoflurane and 250 ml air). All studies were approved by the Experimental Animal Committee of the University of Eastern Finland.

Ovarian cancer was produced by inoculating  $1 \times 10^7$  SKOV-3m cells with 22 G needle into the peritoneal cavity of the nude mice [26]. Development of the tumors was followed by sequential MRI (Figure 1). When the first measurable solid tumor was detected in MRI, gene transfer was performed the following day (day 0) [27]. Mice were randomly divided into four groups: eleven control animals received Ad*LacZ* ( $2 \times 10^9$  pfu) (group I); six animals received combination of AdsVEGFR-2 ( $1 \times 10^9$  pfu) and AdsVEGFR-3 ( $1 \times 10^9$  pfu) (group II); seven animals received the combination of AdsVEGFR-2 ( $1 \times 10^9$  pfu) and AdsVEGFR-3 ( $1 \times 10^9$  pfu) once and after one week a combination of paclitaxel (400  $\mu$ g/ 500  $\mu$ l) and carboplatin (1.6 mg/ 500 $\mu$ l) once (group III); six animals were treated with AdsNRP-1 ( $1 \times 10^9$  pfu) and AdsNRP-2 ( $1 \times 10^9$  pfu) (group IV) (Table 1 and Figure 1).

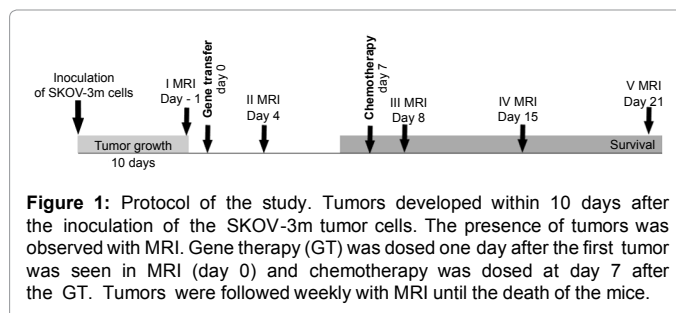


**Figure 1:** Protocol of the study. Tumors developed within 10 days after the inoculation of the SKOV-3m tumor cells. The presence of tumors was observed with MRI. Gene therapy (GT) was dosed one day after the first tumor was seen in MRI (day 0) and chemotherapy was dosed at day 7 after the GT. Tumors were followed weekly with MRI until the death of the mice.

Group	I	II	III	IV
n	11	6	7	6
Adenoviral vector	<i>LacZ</i>	sVEGFR-2	sVEGFR-2	sNRP-1
	-	sVEGFR-3	sVEGFR-3	sNRP-2
Total volume ( $\mu$ l)	200	200	200	200
Titer (pfu/ each vector)	$2 \times 10^9$	$1 \times 10^9$	$1 \times 10^9$	$1 \times 10^9$
Chemotherapy	-	-	Paclitaxel 20 mg/kg	-
	-	-	Carboplatin 80 mg/kg	-

sVEGFR: Soluble Vascular Endothelial Growth Factor Receptor; sNRP: Soluble Neuropilin; Pfu: Plaque-Forming Unit

**Table 1:** Study groups.

Gene transfer was performed intravenously (i.v) via tail vein in the final volume of 200  $\mu$ l in 0.9 % saline, for all vector combinations.

MRI was performed 4, 8, 15 and 21 days after the gene transfer and tumor volumes, ADC values as well as relaxation times  $T_{1\rho}$ ,  $T_2$ ,  $T_{RAFF2}$  and  $T_{RAFF4}$  were measured (Figure 1). The overall follow-up time lasted until emerging of significant symptoms requiring sacrifice or until to the death. At the time of death, the following tissues for further analyses were collected: liver, spleen, kidney, lung, bowel and peritoneum. Also ascites fluid and all tumor tissues were collected and measured.

## Chemotherapy

For chemotherapy paclitaxel infusion concentrate (Paclitaxel Hospira 6 mg/ml; Hospira UK Limited) at a dose of 20 mg/kg and carboplatin concentrate (Carboplatin Hospira 10 mg/ml, Hospira UK Limited) at a dose of 80 mg/kg per mouse was used. Chemotherapy was performed in group III one week after the gene therapy intraperitoneally (i.p.) with 30 G needle (Figure 1). Paclitaxel was dosed before the carboplatin.

## Histology, immunohistochemistry

Tissue samples were immersed in 4 % paraformaldehyde for 4 to 6 h after the autopsy, followed by overnight immersion in 15 % sucrose [35]. Samples were embedded in paraffin and cut to 5  $\mu$ m thick sections (Microtom HM355; Microm) for hematoxylin-eosin, KI-67 (Dako-Cytomation, Glostrup, Denmark) and CD-34 (HyCult Biotech, AA Uden, The Netherlands) stainings. Photographs of histological sections were taken with Olympus AX70 microscope (Olympus Optical, Japan) and processed with AnalySIS (Soft Imaging System, GmbH, Germany) and PhotoShop CS4 (Adobe) softwares. Microvessel density (MVD) and total microvascular area (TVA) of the tumors (%) were measured from CD-34-immunostained sections with AnalySIS software at 100x magnifications in a blinded manner. From each tumor six to 10 different fields were selected to represent maximum MVD areas and necrotic areas were avoided. The findings of the measurements are presented as mean  $\pm$  SEM.

## MRI

All MRI experiments were performed on a horizontal 7 T magnet (Bruker PharmaScan, Bruker BioSpin MRI GmbH, Ettlingen, Germany). For signal transmission and reception, a volume quadrature coil with 40 mm diameter was used (Bruker BioSpin MRI GmbH, Ettlingen, Germany). Animals were anesthetized for MRI with isoflurane inhalation anesthesia (Isoflurane Baxter, Baxter Medical AB) with 4 % initial dose and during imaging the isoflurane level was maintained at 1.5 % in  $\text{NO}_2/\text{O}_2$  (75:25). Respiration was monitored with a pneumatic pillow (SA Instruments, Stony Brook, NY, USA) placed on the mouse abdomen and all imaging was triggered with respiration. The temperature was maintained close to physiological level with a warm water circulating pad. Multislice fast spin echo  $T_2$ -weighted axial images were taken (repetition time (TR) = 3 s, effective echo time (TE) = 44 ms, field of view (FOV) = 40  $\times$  40 mm<sup>2</sup>, matrix size = 256  $\times$  256, slice thickness 1 mm, 30 slices) covering the lower body of the mouse. Using these images, one slice showing the largest tumor in top part of the mice abdomen was selected for the relaxation time measurements and diffusion weighted imaging. The measured relaxation time parameters were the transversal relaxation time  $T_2$  (adiabatic Hahn double echo preparation with TE = 8 - 22 ms), the longitudinal relaxation time in the rotating frame  $T_{1\rho}$  (spin-lock time = 0 - 45.4 ms, RF amplitude ( $\gamma B_1/(2\pi)$ ) = 1250 Hz) [36], and two novel rotating frame parameters; relaxation along a fictitious field in the 2<sup>nd</sup> ( $T_{RAFF2}$ ) and 4<sup>th</sup> frame ( $T_{RAFF4}$ )

( $T_{RAFF2}$  or  $T_{RAFF4}$ -pulses [37,45], pulse train length of 0 - 36 ms,  $\gamma B_1/(2\pi)$  = 1250 Hz for RAFF2 and 648 Hz for RAFF4). The radio frequency field  $B_1$  was measured by incrementing the length of a hard pulse (0.2 - 1.6 ms) placed in front of the readout sequence. For all the relaxation time and  $B_1$  measurements, a fast spin echo sequence was used as readout (TR = 1 s, effective TE = 7.13 ms, FOV = 40  $\times$  40 mm<sup>2</sup>, matrix size = 256  $\times$  256). The apparent diffusion coefficient (ADC) of water was determined by diffusion weighted imaging using a spin echo sequence with diffusion weighting in three orthogonal directions (TR = 1 s, TE = 27 ms, b-value = 0, 500 s/mm<sup>2</sup>, FOV = 40  $\times$  40 mm<sup>2</sup>, matrix size = 128  $\times$  64).

Total tumor volumes from multiple tumor loci (mm<sup>3</sup>) and area of the tumor (mm<sup>2</sup>) were hand drawn on  $T_2$  weighted anatomical images. All relaxation time maps, water ADC-maps and  $B_1$  maps were reconstructed on a pixel-by-pixel basis from the signal intensities. Additionally  $T_{1\rho}$ ,  $T_2$ ,  $T_{RAFF2}$  and  $T_{RAFF4}$  relaxation times and water ADC were analyzed separately for vital and necrotic areas of tumors. All analyses were performed using Aedes software package on Matlab platform (MathWorks, Natick, MA) as in references [28,37]. Tumors were identified from surrounding healthy soft tissue with their deviant intensity and location. Data from all relaxation time measurements were fitted using a single monoexponential decay function. The single cosine function was fitted to  $B_1$  data.

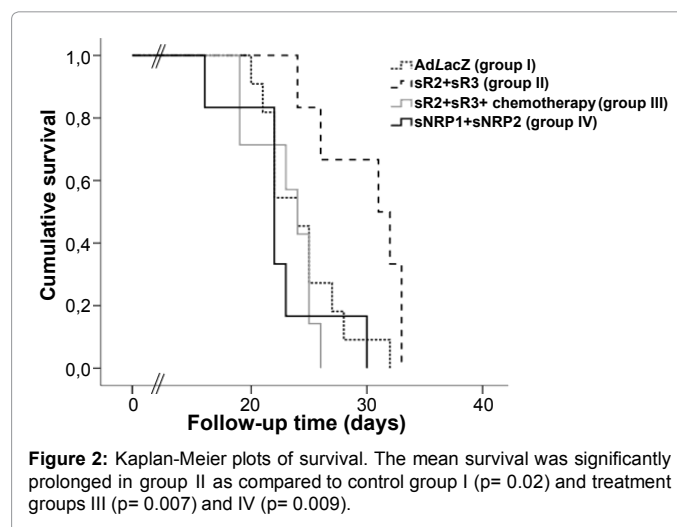
## Statistical analyses

The statistical analyses were performed with IBM SPSS Statistics and Kruskal-Wallis test, followed by Mann-Whitney U test when appropriate. Statistical significance between MRI properties and timepoints was analyzed with mixed model test. For survival analysis Kaplan-Meier plots and log rank test were exploited. Results are shown as mean  $\pm$  SEM. A value of  $p < 0.05$  was considered as statistically significant.

## Results

### Survival

The mean survival was significantly prolonged in group II (30  $\pm$  2 days) compared to control group I (24  $\pm$  1 days,  $p=0.020$ ). In group II, survival was also prolonged compared to the combination of gene therapy and chemotherapy group III (23  $\pm$  1 days,  $p=0.007$ ) and



group IV ( $24 \pm 2$  days,  $p=0.009$ ) (Figure 2). All mice died or they were sacrificed because of the disease and weakness within 33 days.

### Intraperitoneal tumor growth

All mice developed intraperitoneal ovarian cancer tumors within 10 days (6-10 days) after the SKOV-3m cell injections. The progression of tumors was followed with MRI. Although tumor weights were the smallest at the end of the follow-up in gene therapy and chemotherapy combination group III compared to control group I ( $2.8 \pm 0.27$  g versus  $3.4 \pm 0.44$  g; Figure 3a), it did not reach statistical significance.

At the baseline before treatments, the mean tumor volumes detected by MRI were significantly higher in group III ( $290.4 \pm 89.70$  mm<sup>3</sup>) and in group IV ( $398.9 \pm 167.0$  mm<sup>3</sup>) compared to control group I ( $126.9 \pm 40.20$  mm<sup>3</sup>,  $p=0.02$ ;  $p=0.009$ ). By the day 8, the mean tumor volumes decreased from the day 4 values in group II ( $762 \pm 8.70$  mm<sup>3</sup> versus  $578 \pm 141$  mm<sup>3</sup>, 24 %) and group III ( $1040 \pm 112$  mm<sup>3</sup> versus  $1020 \pm 161$  mm<sup>3</sup>, 2.0 %), whereas in control group I the mean tumor volume increased by the day 8 ( $424 \pm 195$  versus  $694 \pm 158$  mm<sup>3</sup>, 55 %). Also, in group IV the mean tumor volume increased from day 4 values ( $818 \pm 258$  mm<sup>3</sup>) by the day 8 ( $1199 \pm 305$  mm<sup>3</sup>, 47 %).

### Formation of ascites

At the end of the follow-up there were no significant differences in the amount of ascitic fluid between the treatment groups (II, III, IV) and control group I (Figure 3b). However, in group III the formation of ascites was lower ( $1.75 \pm 0.72$  ml) than in group II ( $2.59 \pm 0.57$  ml) or group IV ( $2.55 \pm 0.57$  ml). In all treatment groups the formation of ascites was less than in control group I ( $3.58 \pm 1.36$  ml).

### Microvessel measurements

To evaluate the effect of gene therapy and chemotherapy on intratumoral microvessels MVD and TVA (Figures 3c, 3d and 4c) were measured. In group II MVD ( $48.7 \pm 4.50$  /mm<sup>2</sup>) and TVA ( $1.24 \pm 0.11$  %) were significantly smaller compared to control group I ( $84.5 \pm 10.0$  /mm<sup>2</sup>,  $p=0.001$  and  $3.23 \pm 0.70$  %,  $p=0.005$ , respectively) (Figures 3c, 3d and 4c). MVD ( $59.7 \pm 4.20$  /mm<sup>2</sup>) and TVA ( $1.2 \pm 0.10$  %) were significantly smaller also in group III compared to control group I ( $84.5 \pm 10.0$  /mm<sup>2</sup>,  $p=0.002$  and  $3.23 \pm 0.70$  %,  $p=0.003$ , respectively). In group IV MVD ( $62.0 \pm 4.60$  /mm<sup>2</sup>) and TVA ( $1.00 \pm 0.31$  %) were also significantly smaller than in control group I ( $p=0.026$ ;  $p=0.013$ , respectively; Figures 3c, 3d and 4c).

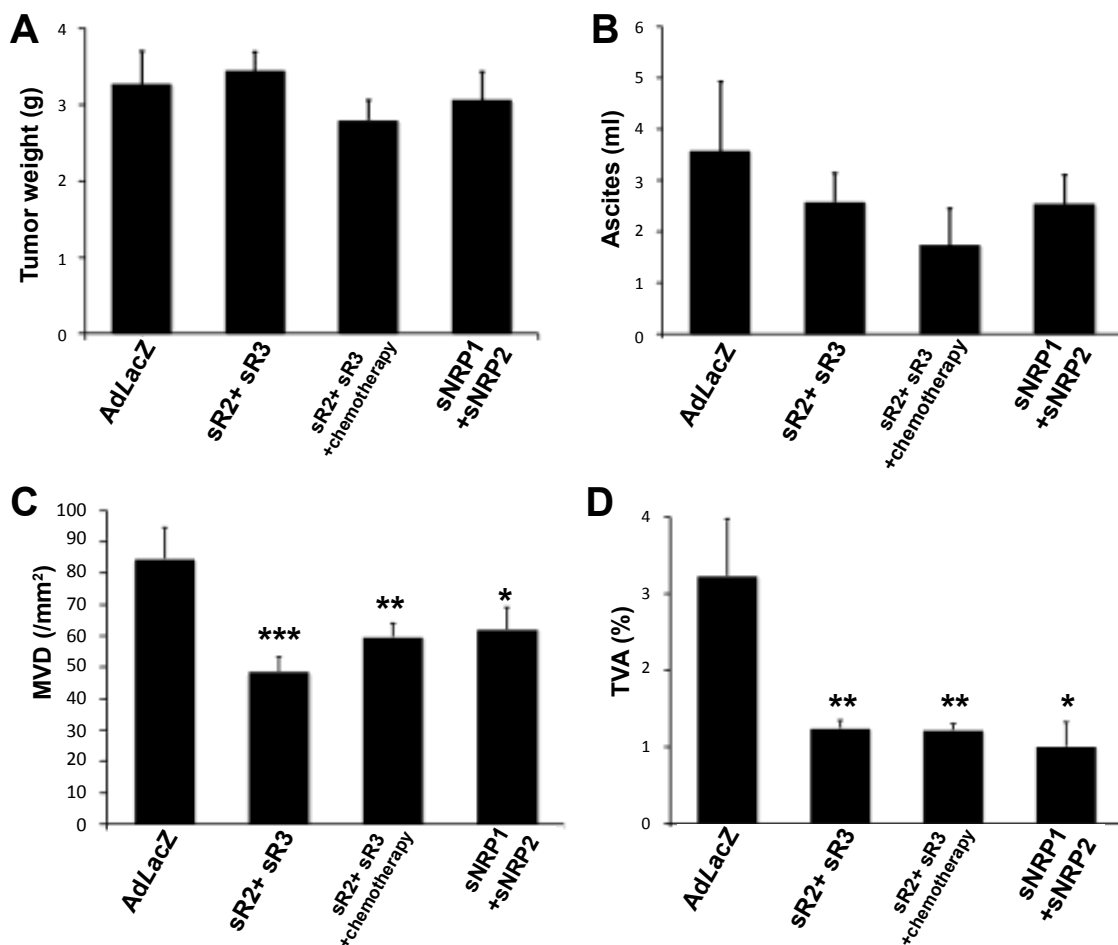


**Figure 3:** Tumor, ascites, microvessel density and total vascular area in the study groups. At the end of the follow up a trend for smaller weights of the tumors (a) and lower amount of ascites (b) was noticed in group III as compared to control group I, although differences were not statistically significant. c) Microvessel density (MVD, microvessels/mm<sup>2</sup>) was significantly reduced in treatment groups II ( $p=0.001$ ), III ( $p=0.002$ ) and IV ( $p=0.026$ ) compared to control group I. d) The total area of microvessels in tumors (TVA, total vascular area) was significantly reduced in treatment groups II ( $p=0.005$ ), III ( $p=0.003$ ) and IV ( $p=0.013$ ) compared to control group I. \* $p < 0.05$ ; \*\* $p < 0.01$ ; \*\*\* $p < 0.001$  versus control group I. Error bars= SEM.

## Histology

Tumors were poorly differentiated high grade serous adenocarcinomas with variable size of nucleus and limited stroma. In all treatment groups II, III and IV, morphology of tumor tissue was partly replaced by fibrosis as compared to control group I (Figure 4a). That was most clearly seen at the end of the follow-up in tumors treated with AdsNRP-1 and AdsNRP-2 (group IV).

Cell proliferation index of tumors measured by KI-67 was significantly lower in group II ( $38.3 \pm 2.80\%$ ) and group III ( $37.1 \pm 4.70\%$ ) compared to control group I ( $67 \pm 4.40\%$ ,  $p=0.002$  and  $p=0.002$  respectively) at the end of the follow-up (Figure 4b).

There were no significant differences in the amount of necrosis in tumors between the control group I ( $30.0 \pm 12.0\%$ ) versus groups II, III or IV ( $28.0 \pm 13.0\%$ ,  $13.0 \pm 4.00\%$ ,  $20.0 \pm 5.00\%$ ; respectively) at the end of the follow-up.

## MRI

From all animals  $T_{1p}$ ,  $T_2$ ,  $T_{RAFF2}$  and  $T_{RAFF4}$  relaxation times and ADC values were analyzed in a slice cut from the centre of an upper part of the abdominal tumor.  $T_2$  relaxation time increased more efficiently in group III at day 4 than in other groups (Figure 5a).  $T_2$  relaxation time was significantly longer at day 8 in group III ( $101 \pm 12.0$  ms) compared to control group I ( $82.0 \pm 7.40$  ms,  $p=0.005$ ) (Figure 5a). A representative graphic of  $T_2$  relaxation time maps is presented in Figure 6. In other relaxation time analyses using  $T_{1p}$ ,  $T_{RAFF2}$  and  $T_{RAFF4}$ , no significant differences between the treatment groups and AdLacZ

controls were observed. The results of all relaxation time analyses are shown in Figure 5.

Water diffusion in tumors was evaluated based on water ADC maps (Figure 7a). Significant transient increase in ADC values was observed at day 4 in group IV ( $1.32 \pm 0.50 \times 10^{-3} \text{ mm}^2/\text{s}$ ) as compared to control group I ( $9.29 \times 10^{-4} \pm 4.10 \times 10^{-5} \text{ mm}^2/\text{s}$ ,  $p=0.044$ ) (Figure 7b). In other treatment groups the ADC was simultaneously decreased at day 4. A representative figure of ADC maps at day 4 of the control group I and treatment group IV is presented in Figure 7a. No significant correlations were noticed between the ADC-values and other MRI parameters at any time points. Results from MRI relaxation time measurements or ADC values did not correlate with survival, tumor size, amount of ascites or with histopathological findings in treatment or in control groups.

At day 8 significant correlations ( $p=0.040$ ,  $r^2=0.54$ ) in  $T_2$  relaxation times between vital ( $84 \pm 7$  ms) and necrotic ( $156 \pm 4.4$  ms) areas were noticed. Also significant positive correlations ( $p=0.007$ ,  $r^2=0.82$ ) at day 4 between vital ( $0.88 \pm 0.07 \times 10^{-3} \text{ mm}^2/\text{s}$ ) and necrotic ( $0.99 \pm 0.14 \times 10^{-3} \text{ mm}^2/\text{s}$ ) areas of ADC values were observed, parallel to day 8 (vital area:  $0.97 \pm 0.09 \times 10^{-3} \text{ mm}^2/\text{s}$  and necrotic area:  $1.05 \pm 0.08 \times 10^{-3} \text{ mm}^2/\text{s}$ ,  $p=0.012$ ,  $r^2=0.63$ ). Also in  $T_{1p}$  relaxation times significant correlations between vital and necrotic areas of tumors (vital area:  $83 \pm 3.5$  ms and necrotic area:  $102 \pm 5.0$  ms,  $p=0.001$ ,  $r^2=0.79$ ) were seen at day 8.  $T_{RAFF2}$  relaxation times in these areas correlated significantly at day 4 (vital area:  $116 \pm 11.7$  ms and necrotic area:  $166 \pm 25.0$  ms,  $p=0.002$ ,  $r^2=0.88$ ) and day 8 (vital area:  $97 \pm 2.0$  and necrotic area:  $121 \pm 3.90$  ms,  $p=0.034$ ,  $r^2=0.57$ ). Additionally  $T_{RAFF4}$  relaxation times in

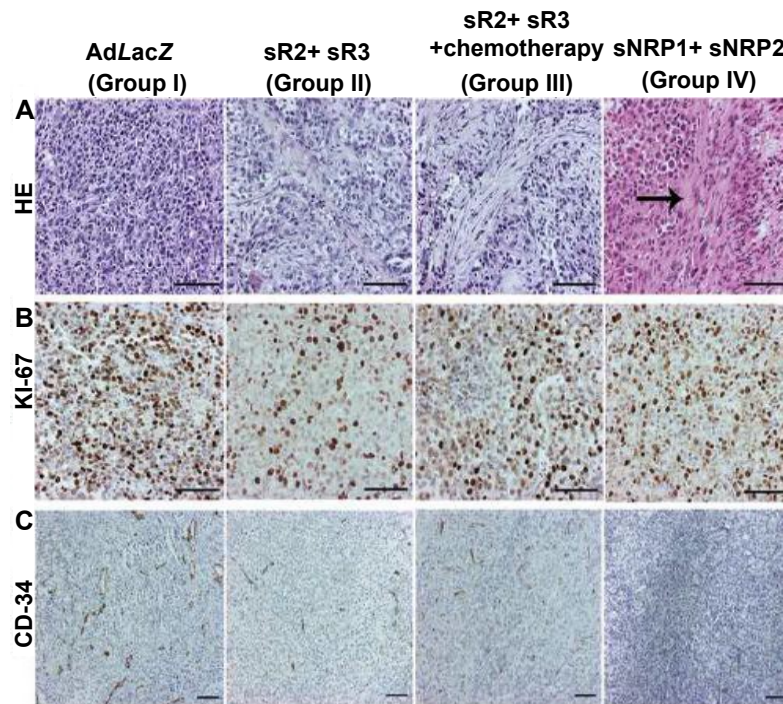


**Figure 4:** Histology of intraperitoneal ovarian cancer tumors. a) Hematoxylin-eosin staining of poorly differentiated high grade serous adenocarcinoma in control group I and treatment groups II, III and IV. Fibrosis (arrow) was most clearly seen in tumors in group IV. b) In KI-67 staining more proliferating tumor cells were noted in control group I compared to groups II ( $p=0.002$ ) and III ( $p=0.002$ ). c) CD-34 positive microvessels in tumor tissues of groups I, II, III and IV. In control group I total vascular area (TVA) was significantly higher than in treatment groups II ( $p=0.005$ ), III ( $p=0.003$ ) or IV ( $p=0.013$ ). Magnification,  $\times 200$  (a-d);  $\times 100$  (e, f). Bar=200  $\mu\text{m}$  or 100  $\mu\text{m}$ .

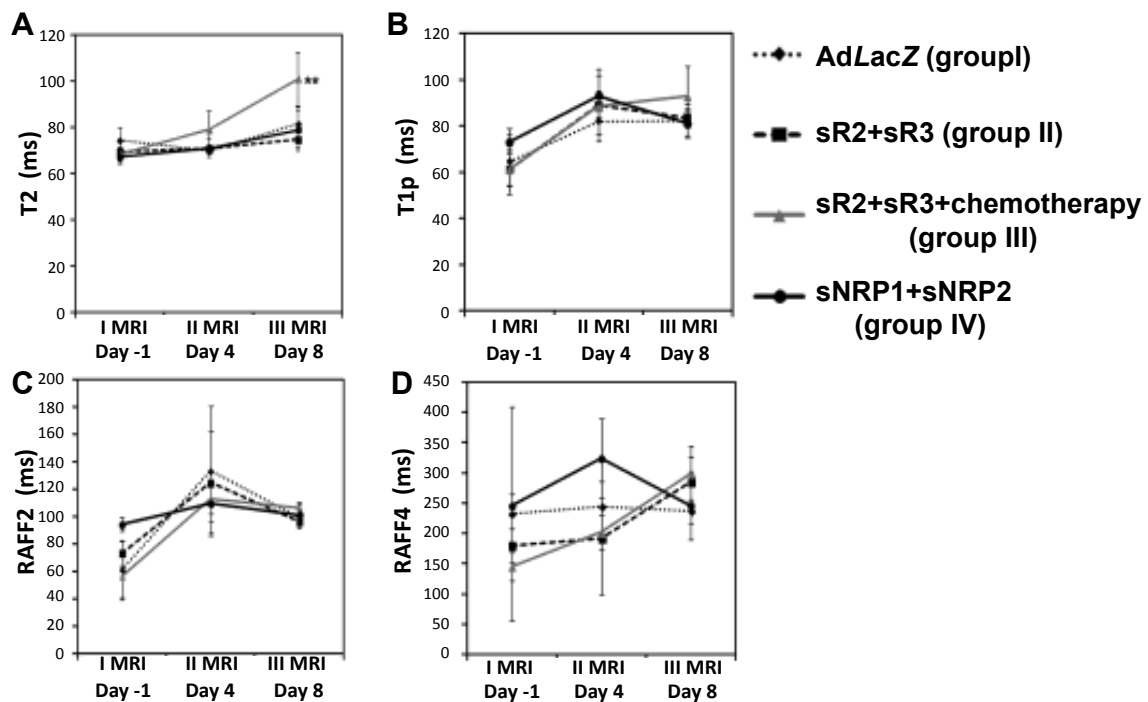


**Figure 5:** Treatment responses evaluated with relaxation times  $T_2$ ,  $T_{1p}$ ,  $T_{RAFF2}$  and  $T_{RAFF4}$  in ovarian cancer tumors at MRI days -1, 4 and 8. a)  $T_2$  relaxation times are significantly longer in combination gene therapy and chemotherapy group III at day 8 ( $p < 0.01$ ) compared with the control group I. b)  $T_{1p}$  relaxation times were increased simultaneously by the day 4 in all groups. c)  $T_{RAFF2}$  and d)  $T_{RAFF4}$  were longer at day 8 compared to levels at the beginning. In other than  $T_2$  relaxation times no significant differences between the treatment groups were noticed. Error bars= SEM.

different areas of tumors correlated significantly at day 8 (vital area:  $276 \pm 29$  ms and necrotic area:  $303 \pm 31.0$  ms,  $p=0.001$ ,  $r^2=0.88$ ).

## Discussion

In this study we present the potential of DW-MRI and relaxation time measurements as early surrogate markers of gene therapy with AdsVEGFR-2 and AdsVEGFR-3 combined with chemotherapy and AdsNRP-1 and AdsNRP-2 gene therapy in ovarian cancer in mice. The present data show that relaxation time  $T_2$  measured by MRI is longer in tumors treated with anti-angiogenic and anti-lymphangiogenic AdsVEGFR-2 and AdsVEGFR-3 gene therapy with chemotherapy (group III) compared to AdLacZ control group I. Alterations in  $T_2$  relaxation time reflect changes in tumor cellularity. Higher ADC values were also observed in treatment group IV as compared to control group I four days after the gene transfer.

In this highly aggressive xenograft model of ovarian cancer the most effective treatment responses were shown in mice that received the combination of gene therapy and paclitaxel and carboplatin chemotherapy according to tumor weights, amount of ascites, microvessel measurements and proliferation index (KI-67) measurements. These results are in line with our previous studies with adenoviral gene therapy with sVEGFR-1, sVEGFR-2 and sVEGFR-3 and a clinical study is warranted [27,29]. Survival was significantly prolonged in treatment group II as compared to control group I and other treatment groups (III, IV). In group III, the mean survival was shorter as compared to the other groups. That might be a result of stressful chemotherapy treatment and disseminated cancer at the time of chemotherapy. According to our preclinical toxicology and biodistribution study, AdsVEGFR-2 and AdsVEGFR-3 gene therapy

was well tolerated even when included in standard chemotherapy with paclitaxel and carboplatin [38].

In preclinical xenograft models of other cancers anti-NRP-1 antibodies have had a modest effect on tumor growth. Anti-NRP-1 antibody is currently in phase I clinical trials with solid malignancies [39]. It has also been reported that anti-NRP-2 has reduced the incidence of lymphatic metastases in a preclinical model [40]. In our ovarian cancer model the antitumor effects were mainly seen in microvessel measurements since MDV and TVA were significantly reduced at the end of the follow-up in treatment group IV. The effects on tumor growth or production of ascites fluid were smaller than in group II.

There is a lack of new reliable surrogate markers and endpoints in the evaluation of the results of current gene therapy trials [9,41]. MRI and DW-MRI related parameters are attractive surrogate markers also for the treatment of cancer since the imaging procedure is non-invasive and does not require either exogenous contrast agents or ionizing radiation. It is important to validate the protocol and indicate the optimal timing for the MRI in animal models of anti-cancer therapies before entering into human studies. As in our previous studies we used the conventional  $T_2$  weighted MRI to detect the intraperitoneal tumor growth before gene therapy. There were significant differences in the size of tumors between the treatment groups 10 days after SKOV-3m cell inoculation reflecting the biological diversity of malignant intraperitoneal ovarian cancer. In this study the MRI was done in several time points to monitor the treatment effects also in the early phase after the therapy, before expected changes in tumor size [20]. Since the treatment protein level in circulation after adenoviral gene therapy rises at highest levels three days after the gene transfer, the first

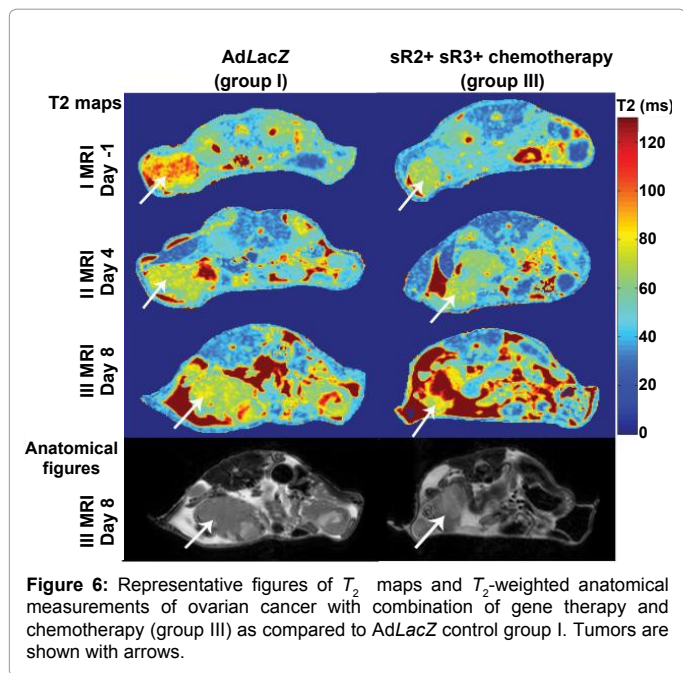


**Figure 6:** Representative figures of  $T_2$  maps and  $T_2$ -weighted anatomical measurements of ovarian cancer with combination of gene therapy and chemotherapy (group III) as compared to AdLacZ control group I. Tumors are shown with arrows.

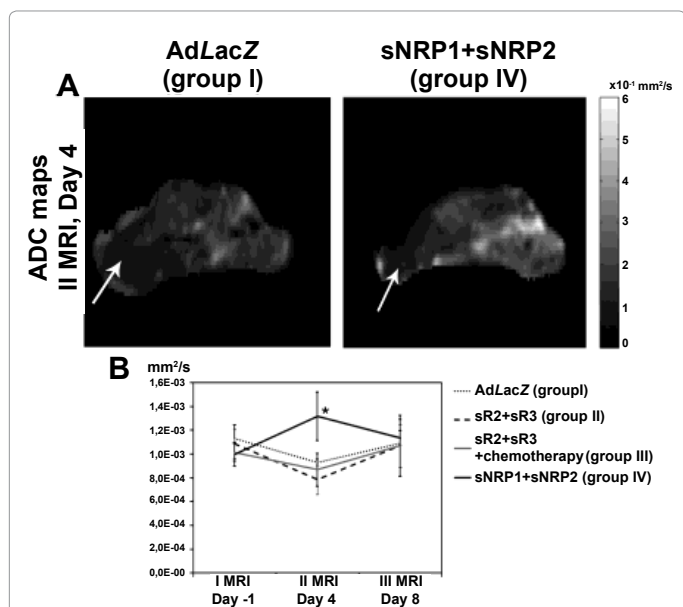


**Figure 7:** a) ADC water diffusion maps at day 4 in control group and group IV. In ADC maps the area of restricted water diffusion and low ADC values appear as darker tone of gray as compared to areas with increased diffusion and lighter tones of gray. b) ADC-values at time points -1, 4 and 8 days. Water diffusion was significantly increased in group IV at day 4 compared to other groups ( $p < 0.05$ ). Tumors are shown with arrows. Error bars= SEM.

time point for imaging responses was four days after the gene transfer [42]. Proliferation index (KI-67) is one of the suggested histological validations of DW-MRI [23]. In present study the proliferation of tumor cells measured by KI-67 staining were significantly reduced in all treatment groups compared to control group I. Unfortunately, the proliferation index did not correlate with any measured MRI parameters.

Increases in ADC values have been noted in several cancer studies

as a result of effective treatments [20,43]. In this study, transient significant increases in ADC values were noticed four days after the AdsNRP-1 and AdsNRP-2 gene therapy (group IV). After that ADC levels declined near to the level of control group I and other treatment groups II, III. Histologically in those tumors the formation of fibrosis was most clearly seen at the end of the follow-up, which may have influenced the different profile of ADC values compared to the other groups. In our study, the ADC values did not correlate with necrosis, although this correlation has been associated previously [43]. Clearly, further studies are needed to better understand the complexity of histological findings and ADC values and to overcome the possible effects of respiratory movements.

$T_2$  relaxation time in tumor tissue was significantly increased in treatment group III eight days after the gene transfer compared to the control group I. Significant prolongation of  $T_2$  relaxation time was noted only in the chemotherapy treated group suggesting the potential of chemotherapy as an enhancer of gene therapy response. In this treatment group the antitumor effects were most clearly seen in tumor growth, ascites formation, microvessels and cell proliferation. The greatest increase in  $T_2$  relaxation times was noticed in necrotic areas of intraperitoneal ovarian tumors as seen in anatomical and diffusion-weighted images, which is in line with earlier results [44]. In clinical studies of brain ischemia, changes in  $T_2$  relaxation time have predicted irreversible cell damage and necrosis in addition to increased ADC values [44]. As a result of anti-angiogenic and anti-lymphangiogenic gene therapy, reduced tumor vascularity and enhanced necrosis, the positive correlations in relaxation times and ADC values between vital and necrotic areas on tumors at days 4 and 8 were expected [45].

$T_1$  relaxation time in the rotating frame ( $T_{1\rho}$ ) is an indicator of acute ischemia since it shows water in close contact with macromolecules and restricted rotation of bulk water [36].  $T_{1\rho}$  with low spin-lock radiofrequency field ( $B_1$ ) is more sensitive than  $T_1$  or  $T_2$  relaxations when detecting the changes in cellularity of tumor border and cytotoxic effects caused by gene therapy in rat malignant glioma model [46]. Changes in  $T_{1\rho}$  relaxation times have been found to occur before the water accumulation and changes in other relaxation time parameters, such as  $T_2$  in cerebral ischemia models, reflecting its potential as an early and sensitive indicator of cell damage [46]. Our results show a trend of increase in  $T_{1\rho}$  times four days after the gene transfer which is in line with results from the rat malignant glioma study, where  $T_{1\rho}$  relaxation time significantly increased four days after the HSV-TK treatment and indicated the cytotoxic effect of gene therapy [22].

To get more comprehensive information from MRI we have measured also novel relaxation time parameters. Relaxation along a fictitious field (RAFF) is a new relaxation time method that may offer a more sensitive marker to evaluate cell density and cell death in different tumor regions as a result of gene therapy as compared to  $T_{1\rho}$  or  $T_2$  weighted imaging [37]. RAFF relaxation times measured in this ovarian cancer model were generally lower corresponding to previous results from the malignant glioma model [24], possibly caused by a more solid mature of the tumor. The wide dispersion seen in  $T_{RAFF4}$  values may be caused by longer  $T_{RAFF4}$  relaxation times compared to  $T_{RAFF2}$  relaxation times, despite the equally long pulse trains used for RAFF weighting or relatively short repetition time (1 sec).

To our knowledge this is the first study to evaluate MRI relaxation time parameters and DW-MRI as early surrogate markers of AdsVEGFR-2 and AdsVEGFR-3 gene therapy alone or with chemotherapy, and AdsNRP-1 and AdsNRP-2 gene therapy in ovarian cancer. We conclude that anti-angiogenic and anti-lymphangiogenic

gene therapy with AdsVEGFR-2 and AdsVEGFR-3 combined with chemotherapy is a potential new treatment for epithelial ovarian cancer in women, and that  $T_2$  relaxation time and ADC are the most potential markers for the evaluation of the early cellular effects of anti-angiogenic gene therapy treatments with MRI.

#### Acknowledgements

We thank Ms. Anneli Miettinen, Ms. Seija Sahrjo, Ms. Sari Järveläinen, Ms. Tiina Koponen and Ms. Helena Kemiläinen for excellent technical assistance. This study was supported by Finnish Academy, The Finnish Medical Foundation, Kuopio University hospital (EVO grant) and Emil Aaltonen Foundation.

#### References

- Jemal A, Bray F, Center MM, Ferlay J, Ward E, et al. (2011) Global cancer statistics. *CA Cancer J Clin* 61: 69-90.
- Heintz AP, Odicino F, Maisonneuve P, Quinn MA, Benedet JL, et al. (2006) Carcinoma of the ovary. FIGO 26th Annual Report on the Results of Treatment in Gynecological Cancer. *Int J Gynaecol Obstet* 95: S161-92.
- Teoh D, Secord AA (2012) Antiangiogenic agents in combination with chemotherapy for the treatment of epithelial ovarian cancer. *Int J Gynecol Cancer* 22: 348-359.
- Hanahan D, Weinberg RA (2000) The hallmarks of cancer. *Cell* 100: 57-70.
- Hefler LA, Zeillinger R, Grimm C, Sood AK, Cheng WF, et al. (2006) Preoperative serum vascular endothelial growth factor as a prognostic parameter in ovarian cancer. *Gynecol Oncol* 103: 512-517.
- Liang B, Guo Z, Li Y, Liu C (2013) Elevated VEGF concentrations in ascites and serum predict adverse prognosis in ovarian cancer. *Scand J Clin Lab Invest*.
- Sowter HM, Corps AN, Evans AL, Clark DE, Charnock-Jones DS, et al. (1997) Expression and localization of the vascular endothelial growth factor family in ovarian epithelial tumors. *Lab Invest* 77: 607-614.
- Olsson AK, Dimberg A, Kreuger J, Claesson-Welsh L (2006) VEGF receptor signalling - in control of vascular function. *Nat Rev Mol Cell Biol* 7: 359-371.
- Ylä-Herttua S, Rissanen TT, Vajanto I, Hartikainen J (2007) Vascular endothelial growth factors: biology and current status of clinical applications in cardiovascular medicine. *J Am Coll Cardiol* 49: 1015-1026.
- Fong GH, Klingensmith J, Wood CR, Rossant J, Breitman ML (1996) Regulation of flt-1 expression during mouse embryogenesis suggests a role in the establishment of vascular endothelium. *Dev Dyn* 207: 1-10.
- Shibuya M (2006) Differential roles of vascular endothelial growth factor receptor-1 and receptor-2 in angiogenesis. *J Biochem Mol Biol* 39: 469-478.
- He Y, Rajantie I, Pajusola K, Jeltsch M, Holopainen T, et al. (2005) Vascular endothelial cell growth factor receptor 3-mediated activation of lymphatic endothelium is crucial for tumor cell entry and spread via lymphatic vessels. *Cancer Res* 65: 4739-4746.
- Laakkonen P, Waltari M, Holopainen T, Takahashi T, Pytowski B, et al. (2007) Vascular endothelial growth factor receptor 3 is involved in tumor angiogenesis and growth. *Cancer Res* 67: 593-599.
- Rossignol M, Gagnon ML, Klagsbrun M (2000) Genomic organization of human neuropilin-1 and neuropilin-2 genes: identification and distribution of splice variants and soluble isoforms. *Genomics* 70: 211-222.
- Staton CA, Kumar I, Reed MW, Brown NJ (2007) Neuropilins in physiological and pathological angiogenesis. *J Pathol* 212: 237-248.
- Kawakami T, Tokunaga T, Hatanaka H, Kijima H, Yamazaki H, et al. (2002) Neuropilin 1 and neuropilin 2 co-expression is significantly correlated with increased vascularity and poor prognosis in non small cell lung carcinoma. *Cancer* 95: 2196-2201.
- Osada H, Tokunaga T, Nishi M, Hatanaka H, Abe Y, et al. (2004) Overexpression of the neuropilin 1 (NRP1) gene correlated with poor prognosis in human glioma. *Anticancer Res* 24: 547-552.
- Hall GH, Turnbull LW, Bedford K, Richmond I, Helboe L, et al. (2005) Neuropilin-1 and VEGF correlate with somatostatin expression and microvessel density in ovarian tumours. *Int J Oncol* 27: 1283-1288.
- Baba T, Kariya M, Higuchi T, Mandai M, Matsumura N, et al. (2007) Neuropilin-1 promotes unlimited growth of ovarian cancer by evading contact inhibition. *Gynecol Oncol* 105: 703-711.
- Chenevert TL, Stegman LD, Taylor JM, Robertson PL, Greenberg HS, et al. (2000) Diffusion magnetic resonance imaging: an early surrogate marker of therapeutic efficacy in brain tumors. *J Natl Cancer Inst* 92: 2029-2036.
- Sugahara T, Korogi Y, Kochi M, Ikushima I, Shigematu Y, et al. (1999) Usefulness of diffusion-weighted MRI with echo-planar technique in the evaluation of cellularity in gliomas. *J Magn Reson Imaging* 9: 53-60.
- Kettunen MI, Sierra A, Närviäinen MJ, Valonen PK, Ylä-Herttua S, et al. (2007) Low spin-lock field T1 relaxation in the rotating frame as a sensitive MR imaging marker for gene therapy treatment response in rat glioma. *Radiology* 243: 796-803.
- Padhani AR, Liu G, Koh DM, Chenevert TL, Thoeny HC, et al. (2009) Diffusion-weighted magnetic resonance imaging as a cancer biomarker: consensus and recommendations. *Neoplasia* 11: 102-125.
- Liimatainen T, Hakumäki JM, Kauppinen RA, Ala-Korpela M (2009) Monitoring of gliomas in vivo by diffusion MRI and  $^1\text{H}$  MRS during gene therapy-induced apoptosis: interrelationships between water diffusion and mobile lipids. *NMR Biomed* 22: 272-279.
- Liimatainen T, Sierra A, Hanson T, Sorce DJ, Ylä-Herttua S, et al. (2012) Glioma cell density in a rat gene therapy model gauged by water relaxation rate along a fictitious magnetic field. *Magn Reson Med* 67: 269-277.
- Sallinen H, Anttila M, Narvainen J, Ordén MR, Ropponen K, et al. (2006) A highly reproducible xenograft model for human ovarian carcinoma and application of MRI and ultrasound in longitudinal follow-up. *Gynecol Oncol* 103: 315-320.
- Sallinen H, Anttila M, Narvainen J, Koponen J, Hamalainen K, et al. (2009) Antiangiogenic gene therapy with soluble VEGFR-1, -2, and -3 reduces the growth of solid human ovarian carcinoma in mice. *Mol Ther* 17: 278-284.
- Sallinen H, Heikura T, Laidinen S, Kosma VM, Heinonen S, et al. (2010) Preoperative angiopoietin-2 serum levels: a marker of malignant potential in ovarian neoplasms and poor prognosis in epithelial ovarian cancer. *Int J Gynecol Cancer* 20: 1498-1505.
- Sopo M, Anttila M, Sallinen H, Tuppurainen L, Laurema A, et al. (2012) Antiangiogenic gene therapy with soluble VEGF-receptors -1, -2 and -3 together with paclitaxel prolongs survival of mice with human ovarian carcinoma. *Int J Cancer* 131: 2394-2401.
- Puumalainen AM, Vapalahti M, Agrawal RS, Kossila M, Laukkanen J, et al. (1998) Beta-galactosidase gene transfer to human malignant glioma in vivo using replication-deficient retroviruses and adenoviruses. *Hum Gene Ther* 9: 1769-1774.
- Roy H, Bhardwaj S, Babu M, Jauhiainen S, Herzig KH, et al. (2005) Adenovirus-mediated gene transfer of placental growth factor to perivascular tissue induces angiogenesis via upregulation of the expression of endogenous vascular endothelial growth factor-A. *Hum Gene Ther* 16: 1422-1428.
- Mäkinen T, Jussila L, Veikkola T, Karpanen T, Kettunen MI, et al. (2001) Inhibition of lymphangiogenesis with resulting lymphedema in transgenic mice expressing soluble VEGF receptor-3. *Nat Med* 7: 199-205.
- Jauhiainen S, Häkkinen SK, Toivanen PI, Heinonen SE, Jyrkkänen HK, et al. (2011) Vascular endothelial growth factor (VEGF)-D stimulates VEGF-A, stanniocalcin-1, and neuropilin-2 and has potent angiogenic effects. *Arterioscler Thromb Vasc Biol* 31: 1617-1624.
- Hedman M, Hartikainen J, Syvanne M, Stjernvall J, Hedman A, et al. (2003) Safety and feasibility of catheter-based local intracoronary vascular endothelial growth factor gene transfer in the prevention of postangioplasty and in-stent restenosis and in the treatment of chronic myocardial ischemia: phase II results of the Kuopio Angiogenesis Trial (KAT). *Circulation* 107: 2677-2683.
- Ylä-Herttua S, Rosenfeld ME, Parthasarathy S, Glass CK, Sigal E, et al. (1990) Colocalization of 15-lipoxygenase mRNA and protein with epitopes of oxidized low density lipoprotein in macrophage-rich areas of atherosclerotic lesions. *Proc Natl Acad Sci U S A* 87: 6959-6963.
- Gröhn OH, Lukkarinen JA, Silvennoinen MJ, Pitkänen A, van Zijl PC, et al. (1999) Quantitative magnetic resonance imaging assessment of cerebral ischemia in rat using on-resonance T(1) in the rotating frame. *Magn Reson Med* 42: 268-276.
- Liimatainen T, Sorce DJ, O'Connell R, Garwood M, Michaeli S (2010) MRI contrast from relaxation along a fictitious field (RAFF). *Magn Reson Med* 64: 983-994.

38. Tuppurainen L, Sallinen H, Kokki E, Koponen J, Anttila M, et al. (2013) Preclinical safety, toxicology, and biodistribution study of adenoviral gene therapy with sVEGFR-2 and sVEGFR-3 combined with chemotherapy for ovarian cancer. *Hum Gene Ther Clin Dev* 24: 29-37.
39. Jubb AM, Strickland LA, Liu SD, Mak J, Schmidt M, et al. (2012) Neuropilin-1 expression in cancer and development. *J Pathol* 226: 50-60.
40. Caunt M, Mak J, Liang WC, Stawicki S, Pan Q, et al. (2008) Blocking neuropilin-2 function inhibits tumor cell metastasis. *Cancer Cell* 13: 331-342.
41. Rätty JK, Liimatainen T, Unelma Kaikkonen M, Gröhn O, Airene KJ, et al. (2007) Non-invasive Imaging in Gene Therapy. *Mol Ther* 15: 1579-1586.
42. Langford G, Dayan A, Yla-Herttuala S, Eckland D (2009) A preclinical assessment of the safety and biodistribution of an adenoviral vector containing the herpes simplex virus thymidine kinase gene (Cerepro) after intracerebral administration. *J Gene Med*. 11: 468-476.
43. Morse DL, Galons JP, Payne CM, Jennings DL, Day S, et al. (2007) MRI-measured water mobility increases in response to chemotherapy via multiple cell-death mechanisms. *NMR Biomed* 20: 602-614.
44. Canese R, Pisanu ME, Mezzanzanica D, Ricci A, Paris L, et al. (2012) Characterisation of in vivo ovarian cancer models by quantitative <sup>1</sup>H magnetic resonance spectroscopy and diffusion-weighted imaging. *NMR Biomed* 25: 632-642.
45. Liimatainen T, Mangia S, Tyan AE, Hakkarainen H, Idiyatullin D, et al. (2013) Generating MRI Contrasts in Rotating Frames of Rank 1 = n = 5 in the Human Brain at 4 T and Mouse Brain at 7 T (4689) Proceedings of 20th Int Soc Magn Reson in Med conference, Melbourne, Australia 2012. (Unpublished).
46. Kettunen MI, Gröhn OH, Penttonen M, Kauppinen RA (2001) Cerebral T1rho relaxation time increases immediately upon global ischemia in the rat independently of blood glucose and anoxic depolarization. *Magn Reson Med* 46: 565-572.

This article was originally published in a special issue, [Cancer Genetics](#) handled by Editor(s), Dr. Ahmed M Malki, Alexandria University, Egypt